THE JOURNAL OF PHYSICAL CHEMISTRY A

Article

Cite This: J. Phys. Chem. A 2018, 122, 6438−6444

pubs.acs.org/JPCA

In Situ Measurement of Exciton Dynamics During Thin-Film Formation Using Single-Shot Transient Absorption

Kelly S. Wilson[†] and Cathy Y. Wong[*,†,‡,§]

[†]Department of Chemistry and Biochemistry, [‡]Oregon Center for Optical, Molecular, and Quantum Science, and [§]Materials Science Institute, University of Oregon, Eugene, Oregon 97403, United States

Supporting Information

ABSTRACT: The exciton dynamics of pseudoisocyanine (PIC) is reported during the formation of a thin film dropcast from solution. Tilted pump pulses are used to spatially encode a pump−probe time delay, enabling the collection of a transient in a single shot. We demonstrate that a spatially encoded delay can be used to accurately measure exciton dynamics in thin-film samples, with a signal-to-noise ratio above 20 attained in 2 s. We report in situ linear absorption, fluorescence, and transient absorption measurements during the molecular aggregation of PIC. These measurements reveal a highly fluorescent intermediate stage during thin-film formation that we ascribe to J-aggregates, in contrast to the final, less fluorescent, dry thin film that exhibits photophysics indicative of disordered J-aggregates. The ability to measure exciton dynamics in situ during materials formation will provide a deeper understanding of how functional materials properties evolve, and will enable direct feedback for rational materials design.

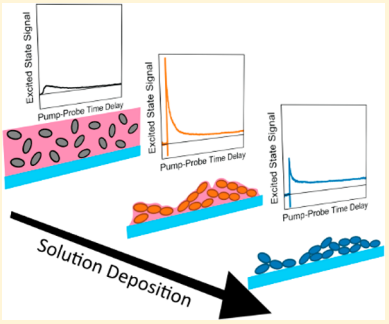

I. INTRODUCTION

The dynamics of bound electron−hole pairs, termed excitons, is important for chemical systems where the fate of excitons determines functionality, such as semiconducting small organic molecules that can serve as the active layer in organic photovoltaics,[1−5] organic electronics,[6−9] and organic light emitting diodes.[10−12] Organic molecules are attractive for these applications since they are synthesized and chemically tunable using earth abundant materials and can be deposited into films from solution using roll-to-roll methods that are scalable for high-volume, low-cost production.[13,14] However, owing to weak intermolecular forces between organic molecules, subtle changes in environmental conditions during the deposition process can affect the relative orientation of molecules within an aggregate, influencing the metastable structures that are kinetically trapped.[15] Since local molecular arrangement determines electronic coupling, and electronic coupling governs electronic structure and exciton dynamics, the aggregate structure can dramatically impact the suitability of a molecule for any particular application. For example, J-aggregates, which are highly fluorescent and useful in light-emitting devices, can form as solvent vaporizes during the solution deposition of an organic molecule such as pseudoisocyanine iodide (PIC). The sharp, red-shifted peak in the linear absorption spectrum of PIC films is ascribed to these J-aggregates, Figure 1a. Multiple experimental and computational studies of the structure of these J-aggregates do not agree,[16,17] suggesting that structure may be sensitive to aggregation conditions. The formation of these J-aggregates can be better understood by measuring the evolving electronic structure and exciton dynamics in situ during aggregate formation.

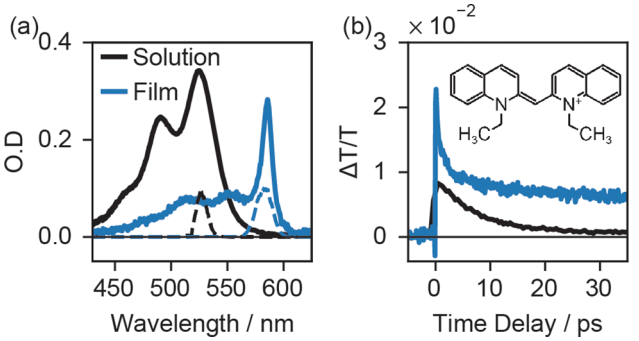

Figure 1. (a) Absorption of PIC (solid) in solution and thin film and laser spectrum (dashed) used for each measurement. (b) TA measurements of PIC in solution and film collected using a translating retroreflector in 13 and 40 min, respectively. Inset: Structure of PIC.

Since linear absorption measurements can be completed quickly (<1 ms) relative to the time scale of film formation (0.1−5 min), in situ measurements can help clarify how the electronic structure evolves during film formation. Exciton dynamics can be measured with femtosecond time resolution using transient absorption (TA) spectroscopy.[18−20] Since the electronic structure clearly changes upon J-aggregate formation, it is unsurprising that the exciton dynamics changes significantly as well, Figure 1b. However, while in situ

Received: June 30, 2018
Published: July 12, 2018

DOI: 10.1021/acs.jpca.8b06248
J. Phys. Chem. A 2018, 122, 6438−6444

measurements of X-ray scattering,[21] linear absorption,[22] nuclear magnetic resonance,[23] and Raman spectroscopy[24] have proliferated, long data collection times have frustrated attempts to use in situ TA spectroscopy to measure the evolution of exciton dynamics during materials formation.

Transient signal is collected by photoexciting the sample using a pump pulse and then measuring the transmission of the excited sample after a controlled time delay using a probe pulse. The time delay is typically controlled using a retroreflecting mirror on a motorized translation stage to vary the path traveled by one of the pulses. Thousands of laser shots are typically used for the transient absorption measurement at each time delay, and the procedure is repeated until an adequate signal-to-noise ratio (SNR) is achieved. This process typically requires many minutes to a few hours. Slowing down the process of film formation would enable the in situ measurement of exciton dynamics, but the structure of the resulting organic molecular aggregates can be extraordinarily sensitive to deposition conditions and the deposition process, as discussed above. Since the electronic structure depends on the aggregate structure, slowing down the aggregation process is not a viable strategy for determining the exciton dynamics during the aggregation of organic molecules. Instead, the measurement must be completed quickly relative to the materials formation process.

We have developed a single-shot transient absorption (SSTA) instrument, described in the Experimental Methods section and shown schematically in Figure 2, that can measure a 45 ps time delay range with excellent SNR in a few seconds.[25] This enables the measurement of exciton dynamics in situ during film formation. The laser spectrum was tuned to overlap with the spectral feature at 583 nm ascribed to J-aggregates,[26−28] Figure 1a. The time delay is spatially encoded within the sample by expanding both the pump and probe beams, using a cylindrical lens to focus each beam to a line on the sample, and tilting the pump pulse relative to the probe pulse. This 45 ps time delay range is, to our knowledge, more than twice as long as any other reported SSTA instrument.[29] This advance is enabled by the use of a spatial light modulator to produce pump pulses that provide even light intensity over the illuminated area.[25] TA instruments reported in literature that use either tilted pulses[30−38] or transmissive/reflective echelons[39−43] to spatially encode the pump−probe time delay have been used to measure exciton dynamics in molecules in solution[25,29,30] and in single crystals[39,40] during photodegradation. Spatially encoded TA has not been used to measure exciton dynamics during film formation, perhaps since it is commonly assumed that spatial encoding cannot accurately measure samples with spatial heterogeneity. In this work, we show that SSTA can accurately measure the ensemble exciton dynamics of a film of PIC molecular aggregates by translating the sample during the measurement to average over heterogeneity. We then use in situ SSTA during the formation of J-aggregates to reveal, for the first time, the exciton dynamics during the film formation process, including the exciton dynamics of an intermediate structure formed prior to the final, dry film. Concurrent in situ linear absorption and fluorescence measurements support an intermediate stage consisting of highly fluorescent J-aggregates with some remaining solvent, while the final stage consists of a dry thin film of disordered, less fluorescent J-aggregates. The insights revealed by measuring practically relevant excitonic processes during materials formation with femtosecond time resolution using in situ SSTA will provide a deeper understanding of how functional materials are formed and enable a more rational approach to excitonic materials design.

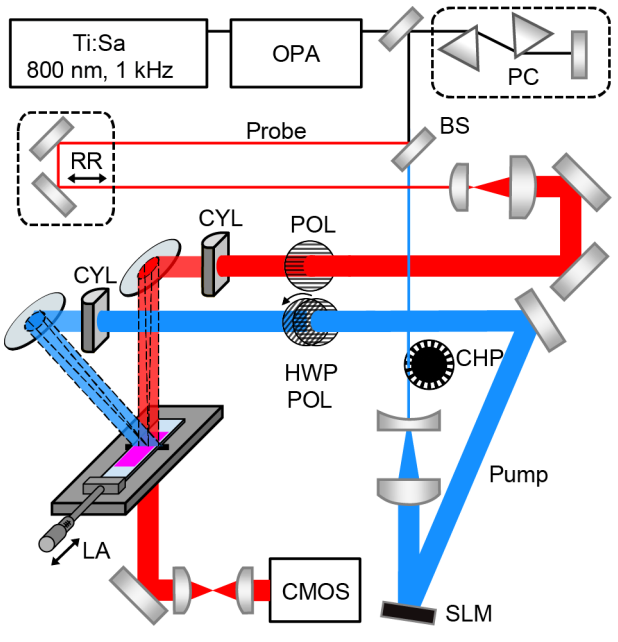

Figure 2. Schematic of SSTA instrument. Key: OPA, optical parametric amplifier; PC, prism compressor; BS, beam splitter; RR, retroreflector; POL, polarizer; CHP, optical chopper; HWP, half-wave plate; SLM, phase-only spatial light modulator; CYL, cylindrical lens; LA, linear actuator; CMOS camera. A thin film is prepared by dropcasting solution onto a glass slide that is translated on a cooled sample stage.

II. EXPERIMENTAL METHODS

SSTA Apparatus. As shown schematically in Figure 2, a 1 kHz Ti:sapphire (Coherent Astrella) laser produces 50 fs pulses that are tuned by an optical parametric amplifier to be resonant with the sample. After a beamsplitter, the probe pulse passes through a beam expander and a retroreflecting mirror mounted on a motorized delay stage (Newport) that is used to calibrate the spatially encoded delay and to collect transients in the traditional manner. The probe beam passes through a cylindrical lens and is normally incident on the sample. The pump pulse passes through a half-wave plate and a polarizer to set the pump:probe energy ratio to 10:1. After an optical chopper and beam expander, the pump interacts with a spatial light modulator (SLM, Meadowlark). An iterative algorithm is used to find a phase map for the SLM that results in a flat intensity profile at the sample position. The pump beam is focused by a cylindrical lens and is tilted by 42.5° relative to the probe pulse.[25] The two beams are overlapped to a 20 mm × 25 μm line on the sample. After passing through the sample, the pump beam is blocked and the probe beam is imaged onto a CMOS camera (Andor Zyla 5.5). A 20 × 2560 image is taken for each shot using a 1 ms exposure time, and each column is summed to generate a 1 × 2560 transmission image, T. The optical chopper blocks alternate pump pulses, and the normalized differential transmission, $\Delta T/T$, is $(T_{\text{pump on}} - T_{\text{pump off}})/T_{\text{pump off}}$.

Power Dependence. When using a spatially encoded time delay, it is important to ensure that the entire measured volume of sample is photoexcited within the linear regime,

DOI: 10.1021/acs.jpca.8b06248
J. Phys. Chem. A 2018, 122, 6438−6444

without interaction between excitons. If one region of the spatial profile of the pump photogenerates a high density of excitons that could annihilate or interact, that spatial region will exhibit exciton dynamics that are different from regions with a lower exciton density. SSTA signals were measured in a PIC film using pulse energies from 0.75 to 2.0 μJ. As shown in Figure S1, the spatially encoded exciton dynamics captured over this range of pump energies is indistinguishable, with a linear dependence of $\Delta T/T$ on pump energy. The pump pulse energy was set to 1.6 μJ for the measurements reported below.

Calibration of the Spatial Time Delay. Concurrent TA and SSTA measurements of a PIC film are used to calibrate the spatial time delay of the instrument. The film is translated during measurement to average over defects like dust particles or scratches. Spatially encoded transient signals are measured at a range of retroreflector positions, Figure 3a. "Time zero", the retroreflector position that results in the overlap of the pump and probe pulses in time, is different for each sample location along the focal line owing to the tilted pump pulse. The relationship between time zero and sample location is very close to linear. A cubic fit of the time zero positions accounts for small deviations from perfectly flat wavefronts and calibrates the pump−probe time delay range to an average of 22.8 fs/pixel.

In Situ Absorption and Fluorescence Measurements. Conjointly with SSTA measurements, in situ absorption and fluorescence measurements are collected via optical fibers (Thorlabs, M28L01) into USB spectrometers (Ocean Optics, Flame-T-VIS-NIR and Flame-T, respectively) with integration times of 280 and 500 ms, respectively. Absorption measurements use a combined light source of a green LED (Uxcell, 510 nm) and a broadband LED (Thorlabs MWWHL3) joined using a bifurcated 6:1 optical fiber (Thorlabs, TP22) and focused at the sample plane. Fluorescence measurements use a 532 nm LED laser excitation source. Because fluorescence measurements are performed concurrently with SSTA, background fluorescence from the ultrafast pulses is also detected. To correct for this, the LED laser is alternately switched on and off every second using a home-built circuit and the measurement with the laser on is subtracted by the in situ background obtained when the laser is off.

PIC Film Deposition and In Situ Measurements. The sample stage consists of an aluminum block with a slot through which the pump and probe pulses can pass, oriented to allow samples to sit horizontally above the measurement slot during thin-film formation. The temperature of the stage is controlled by a recirculating water chiller, in these experiments maintained at 13 °C. A cover is placed over the apparatus to control airflow. A slow flow of nitrogen maintains a 29% humidity level. Microscope slides are sonicated in methanol and dried using nitrogen. PIC is dissolved in acetone through sonication and 0.4 mL are dropcast onto a 2 in. × 1 in. microscope slide on the cooled sample stage. In situ SSTA, absorption and fluorescence measurements, as described above, are initiated simultaneously with dropcasting. Upon formation of the intermediate, a motorized actuator (Newport, TRB25PP) translates the sample at a velocity of 0.3 mm/s until after the final film has formed.

III. RESULTS AND DISCUSSION

Dynamics Measured Using SSTA and TA. Concurrent SSTA and TA measurements of a PIC thin film are used to calibrate the spatial time delay, as described above, and also to ensure that the SSTA instrument accurately measures dynamics of a film with some spatial heterogeneity. Vertical and horizontal slices from Figure 3a correspond to exciton

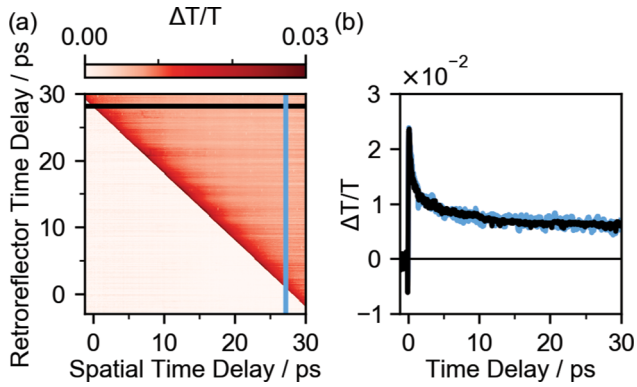

Figure 3. Comparison of SSTA and traditional TA measurements of PIC. (a) SSTA measurements taken over a range of time delays generated by translating a retroreflector. (b) Slices from (a) show comparable exciton dynamics measured using traditional TA and SSTA collected in 14 min and 2 s, respectively.

dynamics measured by translating the retroreflector and by using the spatially encoded time delay, respectively. The dynamics measured by translating a retroreflector agrees with the dynamics measured using the spatially encoded time delay, Figure 3b, demonstrating the accuracy of the SSTA instrument. Using the spatially encoded time delay a SNR > 20 can be achieved in 2 s, enabling the measurement of exciton dynamics in molecules as they aggregate to form films. The acquisition time and film area needed to average over spatial heterogeneity will depend on the degree and type of heterogeneity in the sample.

In Situ Measurements of PIC Films during Formation. The process of PIC film formation occurs in ∼30 s using our deposition method and conditions. In situ linear absorption, fluorescence, and SSTA were measured during the thin-film formation process, Figure 4. The plot of linear absorption as a function of real time, Figure 4a, shows that molecular aggregation proceeds through three distinct stages, which we term the "solution", "intermediate", and "film" stages, with clear changes in the spectral features at 0 and ∼20 s. In this work, we focus on the J-aggregates, which produce the strong, narrow absorption feature at 583 nm during the intermediate stage, between 0 and 20 s. This feature then broadens and slightly red-shifts when it has formed a film, Figure 5. Absorption spectra collected during the solution, intermediate, and film stages are compared in Figure 4b. The three stages of the aggregation process are also evident in the fluorescence spectra, Figure 4c. In solution, the fluorescence is below the detection limit of our instrument. Upon formation of the intermediate stage, the film becomes highly fluorescent at 583 nm. After undergoing the transition to the final film, the fluorescence intensity decreases, the spectrum slightly red-shifts to 585 nm, both shown in Figure 4d, and the line width broadens, Figure 5.

SSTA was measured during film formation using laser pulses centered at 583 nm, resonant with the narrow band arising from J-aggregates. The exciton dynamics during the intermediate stage is clearly different from the dynamics measured in the film stage, as shown in Figure 4e, where each SSTA transient is the average of 500 shots collected in 1 s

DOI: 10.1021/acs.jpca.8b06248
J. Phys. Chem. A 2018, 122, 6438−6444

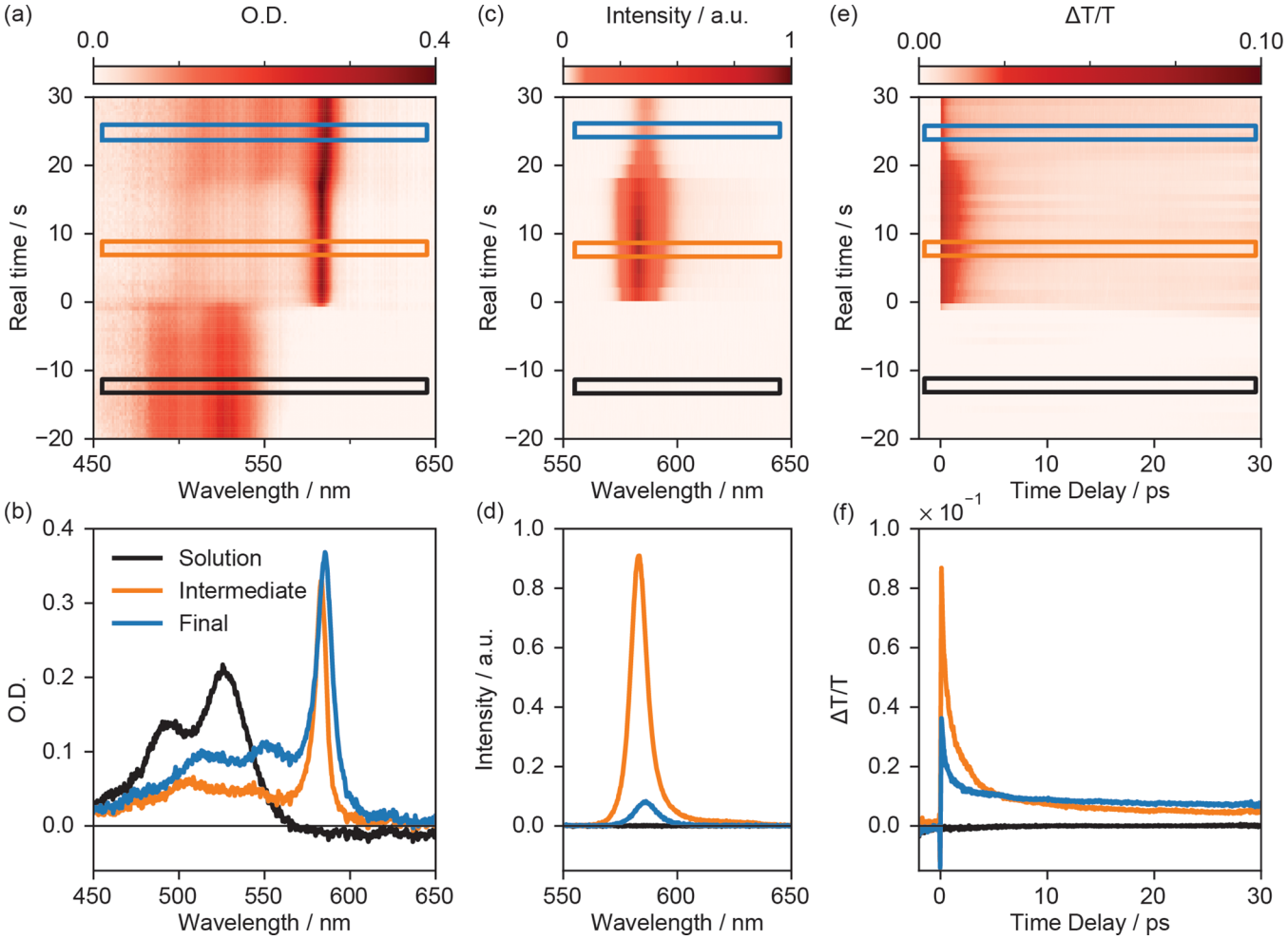

Figure 4. In situ measurements of (a, b) absorption, (c, d) fluorescence, and (e, f) SSTA during molecular aggregation into a film. (b) Absorption, (d) fluorescence, and (f) SSTA measurements collected during the solution, intermediate, and final stages. Colored lines in (a, c, e) indicate the real time of data in (b, d, f). The one-color SSTA measurements were performed using the laser spectrum shown in Figure 1a centered at 583 nm.

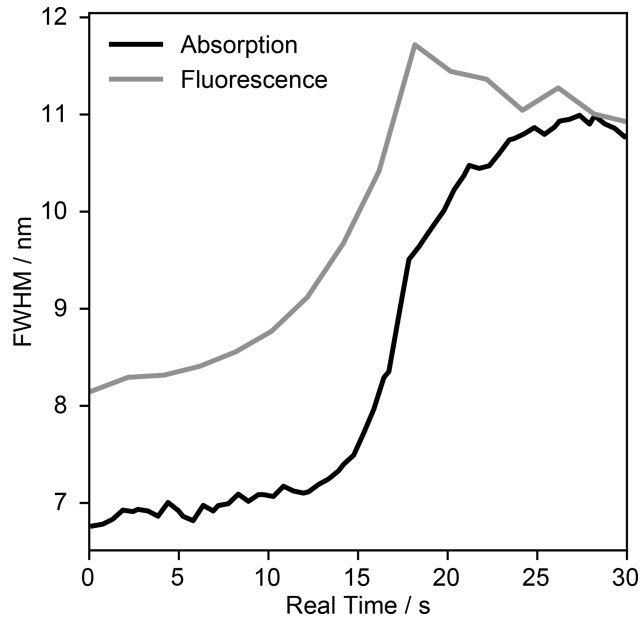

Figure 5. Full width at half-maximum (FWHM) of the J-aggregate absorbance and fluorescence features measured in situ during the intermediate and final stages.

while translating over a 12 mm × 0.3 mm area of sample. Figure 4f compares transients collected during the intermediate and film stages. The TA signal immediately after photoexcitation is larger in magnitude during the intermediate stage than in the film stage, but both signals decay to the same magnitude by 10 ps. The TA signal collected during the intermediate stage can be fit using a biexponential function and a constant offset, $\Delta T/T = a_1 \exp(-t/\tau_1) + a_2 \exp(-t/\tau_2) + a_3$. This function cannot fit the TA signal collected during the film stage, and a triexponential must be employed, $\Delta T/T = a_1 \exp(-t/\tau_1) + a_2 \exp(-t/\tau_2) + a_3 \exp(-t/\tau_3)$. A rolling average of TA signal collected over 6 s was used for each fit. The shortest decay constant extracted from the fits of TA signal collected during the intermediate stage was statistically indistinguishable from that of the final stage, with an average of $\tau_1 = 0.31 \pm 0.06$ ps. Similarly, the second shortest time constant extracted from fits of both the intermediate and film stages are similar, with an average of $\tau_2 = 2.55 \pm 0.53$ ps. Since these two time constants remain the same as the sample evolves from the intermediate stage to the film stage, it is likely that the fast physical processes that result in these two exponential signal decays do not change. This is not the case for the longer physical processes. While the long-lived TA signal collected during the intermediate stage is well fit by a constant offset, a third exponential function must be used to fit

DOI: 10.1021/acs.jpca.8b06248
J. Phys. Chem. A 2018, 122, 6438−6444

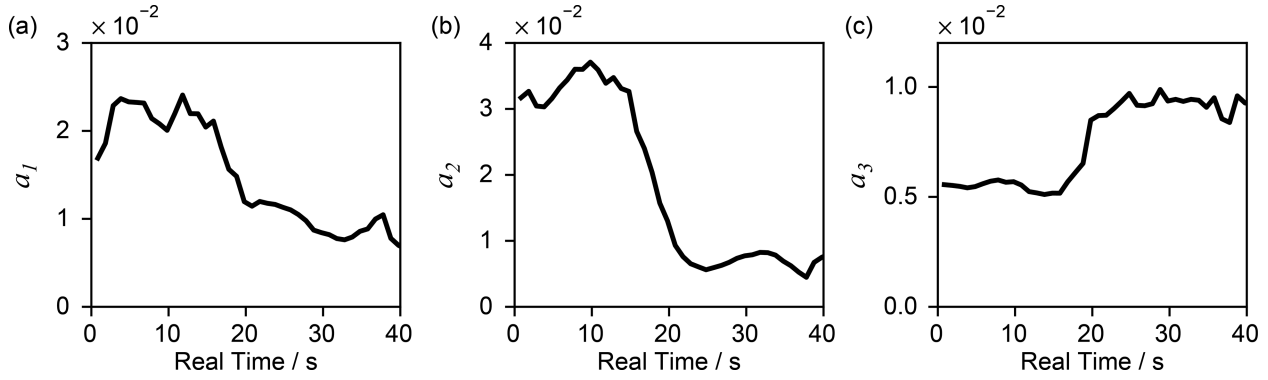

Figure 6. Amplitudes of the three exponentials used to fit the transients collected in situ during the intermediate and final stages.

the signal collected during the film stage, with a time constant of τ_3 = 96.7 ± 16.0 ps. This change indicates the emergence of a new, faster, physical process to return excitons to the ground state when the sample transitions from the intermediate stage to the film stage. The decrease in fluorescence intensity suggests that this faster process is nonradiative and outcompetes the radiative process that is more prevalent during the intermediate stage. The evolution of the corresponding amplitudes for each of the time constants in the fits is shown in Figure 6. The transition from the intermediate to the final stage is apparent at ∼20 s. The contribution of the two faster exponential decays to the overall SSTA transient signal decreases as the sample transitions from the intermediate stage to the film, while the amplitude of the long-lived component increases. It is notable that these dramatic changes in the fluorescence intensity and the exciton dynamics are not matched by a dramatic change in the absorption line shape. The red shift of the three distinct peaks in the absorption spectrum and the change in their peak intensity ratios upon transition from the intermediate stage to the film stage are quite subtle by comparison, shown in Figure S3. The increased line width of the J-aggregate absorption and fluorescence peaks upon transition to the film stage, shown in Figure 5, suggests that the aggregates in the film are more disordered, potentially as a result of the vaporization of the last shell of solvent around the aggregates. Without a solvent shell, the aggregates will physically contact each other, potentially disrupting individual aggregate structures. This may introduce a fast quenching pathway and reduce the number of aggregates that fluoresce. This picture agrees with the measurements of Sorokin et al., who report that topological disorder and exciton−phonon coupling result in exciton self-trapping in films of PIC, observed as an increase in nonradiative relaxation and decrease in the luminescence quantum yield.[44] Photoluminescence measurements of PIC aggregates in solution by Cooper also support this picture.[45] The fluorescence band was observed to split into two peaks at cryogenic temperatures. Fidder later supported Cooper's findings and found that the two aggregate structures with different fluorescence yields can coexist within the same aggregate chain.[46] This suggests that multiple aggregate structures may be able to form and coexist when the aggregates contact each other as the final solvent shell is removed. The absorption and fluorescence peak positions and intensities will be different for each aggregate structure owing to the sensitivity of electronic structure to the precise arrangement of molecules. As the final solvation shell is stripped from the aggregates during the transition of our films from the intermediate stage to the final stage, it is possible that multiple aggregate structures are formed, resulting in spectral features that are broader and slightly shifted. A deeper analysis of the mechanism of fluorescence quenching is currently being pursued. Further experiments using in situ grazing incidence wide-angle X-ray scattering during film formation could help distinguish the structure difference between the intermediate and final film structures.[47,48]

IV. CONCLUSION

For the first time, exciton dynamics has been revealed during thin-film formation by translating the thin film during SSTA measurements to average over heterogeneity. Future studies will explore the impact of heterogeneity on SSTA measurements and develop methods for detecting and filtering out severe heterogeneity. We reveal an intermediate stage during the film formation process that persists for approximately 20 s. The exciton dynamics during this stage of aggregation cannot be probed without SSTA. These data, in conjunction with in situ absorption and fluorescence, provide insight into the electronic structure and exciton dynamics of materials that are not at structural equilibrium. The ability to measure properties that directly determine material functionality in situ during materials formation will provide valuable feedback for the rational design of functional excitonic materials. Understanding the evolution of exciton dynamics during the formation of organic molecular aggregates, the self-assembly of arrays of nanocrystals, or during chemical reactions will provide insight into how materials with a particular photophysics can be kinetically trapped.

■ ASSOCIATED CONTENT

Supporting Information

The Supporting Information is available free of charge on the ACS Publications website at DOI: 10.1021/acs.jpca.8b06248.

Power dependence of SSTA signal; impact of sample translation during measurement; absorbance and fluorescence peak wavelength and intensities during deposition (PDF)

■ AUTHOR INFORMATION

Corresponding Author

*C. Y. Wong. cwong3@uoregon.edu.

ORCID

Cathy Y. Wong: 0000-0001-6867-1968

Notes

The authors declare no competing financial interest.

DOI: 10.1021/acs.jpca.8b06248
J. Phys. Chem. A 2018, 122, 6438−6444

■ ACKNOWLEDGMENTS

This material is based upon work supported by the National Science Foundation under Grant No. 1752129.

■ REFERENCES

(1) Darling, S. B.; You, F. The Case for Organic Photovoltaics. *RSC Adv.* **2013**, *3*, 17633−17648.
(2) Janssen, R. A. J.; Nelson, J. Factors Limiting Device Efficiency in Organic Photovoltaics. *Adv. Mater.* **2013**, *25*, 1847−1858.
(3) Walker, B.; Kim, C.; Nguyen, T.-Q. Small Molecule Solution-Processed Bulk Heterojunction Solar Cells. *Chem. Mater.* **2011**, *23*, 470−482.
(4) Mishra, A.; Baeuerle, P. Small Molecule Organic Semiconductors on the Move: Promises for Future Solar Energy Technology. *Angew. Chem., Int. Ed.* **2012**, *51*, 2020−2067.
(5) Brédas, J.-L.; Norton, J. E.; Cornil, J.; Coropceanu, V. Molecular Understanding of Organic Solar Cells: The Challenges. *Acc. Chem. Res.* **2009**, *42*, 1691−1699.
(6) Sirringhaus, H. 25th Anniversary Article: Organic Field-Effect Transistors: The Path Beyond Amorphous Silicon. *Adv. Mater.* **2014**, *26*, 1319−1335.
(7) Anthony, J. E.; Facchetti, A.; Heeney, M.; Marder, S. R.; Zhan, X. N-Type Organic Semiconductors in Organic Electronics. *Adv. Mater.* **2010**, *22*, 3876−3892.
(8) Figueira-Duarte, T. M.; Muellen, K. Pyrene-Based Materials for Organic Electronics. *Chem. Rev.* **2011**, *111*, 7260−7314.
(9) Kim, F. S.; Ren, G.; Jenekhe, S. A. One-Dimensional Nanostructures of Pi-Conjugated Molecular Systems: Assembly, Properties, and Applications from Photovoltaics, Sensors, and Nanophotonics to Nanoelectronics. *Chem. Mater.* **2011**, *23*, 682−732.
(10) Mei, J.; Hong, Y.; Lam, J. W. Y.; Qin, A.; Tang, Y.; Tang, B. Z. Aggregation-Induced Emission: The Whole Is More Brilliant than the Parts. *Adv. Mater.* **2014**, *26*, 5429−5479.
(11) Zhong, C.; Duan, C.; Huang, F.; Wu, H.; Cao, Y. Materials and Devices toward Fully Solution Processable Organic Light-Emitting Diodes. *Chem. Mater.* **2011**, *23*, 326−340.
(12) Thejo Kalyani, N.; Dhoble, S. J. Organic Light Emitting Diodes: Energy Saving Lighting Technology—A Review. *Renewable Sustainable Energy Rev.* **2012**, *16*, 2696−2723.
(13) Liu, K.; Trofod Larsen-Olsen, T.; Lin, Y.; Beliatis, M.; Bundgaard, E.; Jørgensen, M.; Krebs, F. C.; Zhan, X. Roll-Coating Fabrication of Flexible Organic Solar Cells: Comparison of Fullerene and Fullerene-Free Systems. *J. Mater. Chem. A* **2016**, *4*, 1044−1051.
(14) Sondergaard, R. R.; Hosel, M.; Krebs, F. C. Roll-to-Roll Fabrication of Large Area Functional Organic Materials. *J. Polym. Sci., Part B: Polym. Phys.* **2013**, *51*, 16−34.
(15) Giri, G.; Verploegen, E.; Mannsfeld, S. C. B.; Atahan-Evrenk, S.; Kim, D. H.; Lee, S. Y.; Becerril, H. A.; Aspuru-Guzik, A.; Toney, M. F.; Bao, Z. Tuning Charge Transport in Solution-Sheared Organic Semiconductors Using Lattice Strain. *Nature* **2011**, *480*, 504−508.
(16) Haverkort, F.; Stradomska, A.; Knoester, J. First-Principles Simulations of the Initial Phase of Self-Aggregation of a Cyanine Dye: Structure and Optical Spectra. *J. Phys. Chem. B* **2014**, *118*, 8877−8890.
(17) Würthner, F.; Kaiser, T. E.; Saha-Möller, C. R. J-Aggregates: From Serendipitous Discovery to Supramolecular Engineering of Functional Dye Materials. *Angew. Chem., Int. Ed.***2011***50*, 3376−3410.
(18) Pollard, W. T.; Mathies, R. A. Analysis of Femtosecond Dynamic Absorption Spectra of Nonstationary States. *Annu. Rev. Phys. Chem.* **1992**, *43*, 497−523.
(19) Lanzani, G. Pump Probe and Other Modulation Techniques. In *The Photophysics Behind Photovoltaics and Photonics*; Wiley-VCH Verlag GmbH & Co. KGaA., 2012; p 177.
(20) Megerle, U.; Pugliesi, I.; Schriever, C.; Sailer, C. F.; Riedle, E. Sub-50 Fs Broadband Absorption Spectroscopy with Tunable Excitation: Putting the Analysis of Ultrafast Molecular Dynamics on Solid Ground. *Appl. Phys. B: Lasers Opt.* **2009**, *96*, 215−231.
(21) Giri, G.; Li, R.; Smilgies, D.-M.; Li, E. Q.; Diao, Y.; Lenn, K. M.; Chiu, M.; Lin, D. W.; Allen, R.; Reinspach, J.; et al. One-Dimensional Self-Confinement Promotes Polymorph Selection in Large-Area Organic Semiconductor Thin Films. *Nat. Commun.* **2014**, *5*, 3575.
(22) Hernandez, J. L.; Reichmanis, E.; Reynolds, J. R. Probing Film Solidification Dynamics in Polymer Photovoltaics. *Org. Electron.* **2015**, *25*, 57−65.
(23) Griffin, J. M.; Forse, A. C.; Tsai, W.-Y.; Taberna, P.-L.; Simon, P.; Grey, C. P. *In Situ* NMR and Electrochemical Quartz Crystal Microbalance Techniques Reveal the Structure of the Electrical Double Layer in Supercapacitors. *Nat. Mater.* **2015**, *14*, 812−820.
(24) Frank, O.; Dresselhaus, M. S.; Kalbac, M. Raman Spectroscopy and in Situ Raman Spectroelectrochemistry of Isotopically Engineered Graphene Systems. *Acc. Chem. Res.* **2015**, *48*, 111−118.
(25) Wilson, K. S.; Wong, C. Y. Single-Shot Transient Absorption Spectroscopy with a 45 Ps Pump-Probe Time Delay Range. *Opt. Lett.* **2018**, *43*, 371−374.
(26) Kopainsky, B.; Kaiser, W. Ultrafast Transient Processes of Monomers, Dimers, and Aggregates of Pseudoisocyanine Chloride (PIC). *Chem. Phys. Lett.* **1982**, *88*, 357−361.
(27) Struganova, I. Dynamics of Formation of 1,1′-Diethyl-2,2′-Cyanine Iodide J-Aggregates in Solution. *J. Phys. Chem. A* **2000**, *104*, 9670−9674.
(28) Neumann, B. On the Aggregation Behavior of Pseudoisocyanine Chloride in Aqueous Solution as Probed by UV/Vis Spectroscopy and Static Light Scattering. *J. Phys. Chem. B* **2001**, *105*, 8268−8274.
(29) Minami, Y.; Yamaki, H.; Katayama, I.; Takeda, J. Broadband Pump−Probe Imaging Spectroscopy Applicable to Ultrafast Single-Shot Events. *Appl. Phys. Express* **2014**, *7*, 022402.
(30) Dhar, L.; Fourkas, J. T.; Nelson, K. A. Pulse-Length-Limited Ultrafast Pump−Probe Spectroscopy in a Single Laser Shot. *Opt. Lett.* **1994**, *19*, 643−645.
(31) Salin, F.; Georges, P.; Roger, G.; Brun, A. Single-Shot Measurement of a 52-fs Pulse. *Appl. Opt.* **1987**, *26*, 4528−4531.
(32) Fourkas, J. T.; Dhar, L.; Nelson, K. A.; Trebino, R. Spatially Encoded, Single-Shot Ultrafast Spectroscopies. *J. Opt. Soc. Am. B* **1995**, *12*, 155−165.
(33) Weinkauf, R.; Lehr, L.; Georgiev, D.; Schlag, E. W. Time Multiplexing: A New Single Shot Femtosecond Pump-Probe Technique. *Appl. Phys. B: Lasers Opt.* **1997**, *64*, 515−519.
(34) Fujimoto, M.; Aoshima, S.; Tsuchiya, Y. Ultrafast Imaging to Measure Instantaneous Intensity Distributions of Femtosecond Optical Pulses Propagating in a Medium. *Meas. Sci. Technol.* **2002**, *13*, 1698.
(35) Furukawa, N.; Mair, C. E.; Kleiman, V. D.; Takeda, J. Femtosecond Real-Time Pump−Probe Imaging Spectroscopy. *Appl. Phys. Lett.* **2004**, *85*, 4645−4647.
(36) Makishima, Y.; Furukawa, N.; Ishida, A.; Takeda, J. Femtosecond Real-Time Pump-Probe Imaging Spectroscopy Implemented on a Single Shot Basis. *Jpn. J. Appl. Phys.* **2006**, *45*, 5986.
(37) Ferrari, R.; D'Andrea, C.; Bassi, A.; Valentini, G.; Cubeddu, R. Time-Gated Real-Time Pump-Probe Imaging Spectroscopy. In Novel Optical Instrumentation for Biomedical Applications III 2007. *Proc. SPIE* **2007**, 663118.
(38) Harel, E.; Fidler, A. F.; Engel, G. S. Single-Shot Gradient-Assisted Photon Echo Electronic Spectroscopy. *J. Phys. Chem. A* **2011**, *115*, 3787−3796.
(39) Poulin, P. R.; Nelson, K. A. Irreversible Organic Crystalline Chemistry Monitored in Real Time. *Science* **2006**, *313*, 1756−1760.
(40) Wakeham, G. P.; Nelson, K. A. Dual-Echelon Single-Shot Femtosecond Spectroscopy. *Opt. Lett.* **2000**, *25*, 505−507.
(41) Shin, T.; Wolfson, J. W.; Teitelbaum, S. W.; Kandyla, M.; Nelson, K. A. Dual Echelon Femtosecond Single-Shot Spectroscopy. *Rev. Sci. Instrum.* **2014**, *85*, 083115.
(42) Sakaibara, H.; Ikegaya, Y.; Katayama, I.; Takeda, J. Single-Shot Time-Frequency Imaging Spectroscopy Using an Echelon Mirror. *Opt. Lett.* **2012**, *37*, 1118−1120.

DOI: 10.1021/acs.jpca.8b06248
J. Phys. Chem. A 2018, 122, 6438−6444

(43) Aagedal, H.; Schmid, M.; Egner, S.; Müller-Quade, J.; Beth, T.; Wyrowski, F. Analytical Beam Shaping with Application to Laser-Diode Arrays. *J. Opt. Soc. Am. A* **1997**, *14*, 1549−1553.
(44) Sorokin, A. V.; Pereverzev, N. V.; Grankina, I. I.; Yefimova, S. L.; Malyukin, Y. V. Evidence of Exciton Self-Trapping in Pseudoisocyanine J-Aggregates Formed in Layered Polymer Films. *J. Phys. Chem. C* **2015**, *119*, 27865−27873.
(45) Cooper, W. Multiplet Structure of Aggregated States in 1,1-Diethyl-2,2-Cyanine Dye. *Chem. Phys. Lett.* **1970**, *7*, 73−77.
(46) Fidder, H. Absorption and Emission Studies on Pure and Mixed J-Aggregates of Pseudoisocyanine. *Chem. Phys.* **2007**, *341*, 158−168.
(47) Smilgies, D.-M.; Li, R.; Giri, G.; Chou, K. W.; Diao, Y.; Bao, Z.; Amassian, A. Look Fast: Crystallization of Conjugated Molecules during Solution Shearing Probed in-Situ and in Real Time by X-Ray Scattering. Phys. *Phys. Status Solidi RRL* **2013**, *7*, 177−179.
(48) Li, R.; Khan, H. U.; Payne, M. M.; Smilgies, D.-M.; Anthony, J. E.; Amassian, A. Heterogeneous Nucleation Promotes Carrier Transport in Solution-Processed Organic Field-Effect Transistors. *Adv. Funct. Mater.* **2013**, *23*, 291−297.

DOI: 10.1021/acs.jpca.8b06248
J. Phys. Chem. A 2018, 122, 6438−6444